

BLACK HOLES

A precise measurement of the magnetic field in the corona of the black hole binary V404 Cygni

Yigit Dallilar,^{1*} Stephen S. Eikenberry,^{1*} Alan Garner,¹ Richard D. Stelter,¹ Amy Gottlieb,¹ Poshak Gandhi,² Piergiorgio Casella,³ Vik S. Dhillon,^{4,5} Tom R. Marsh,⁶ Stuart P. Littlefair,⁴ Liam Hardy,⁴ Rob Fender,⁷ Kunal Mooley,⁷ Dominic J. Walton,⁸ Felix Fuerst,^{9,10} Matteo Bachetti,¹¹ A. J. Castro-Tirado,^{12,13} Miguel Charcos,¹ Michelle L. Edwards,¹⁴ Nestor M. Lasso-Cabrera,¹⁵ Antonio Marin-Franch,¹⁵ S. Nicholas Raines,¹ Kendall Ackley,¹ John G. Bennett,¹ A. Javier Cenarro,¹⁵ Brian Chinn,¹ H. Veronica Donoso,¹ Raymond Frommeyer,^{1†} Kevin Hanna,¹ Michael D. Herlevich,¹ Jeff Julian,¹ Paola Miller,¹ Scott Mullin,¹ Charles H. Murphey,¹ Chris Packham,^{16,17} Frank Varosi,¹ Claudia Vega,¹ Craig Warner,¹ A. N. Ramaprakash,¹⁸ Mahesh Burse,¹⁸ Sujit Punnadi,¹⁸ Pravin Chordia,¹⁸ Andreas Gerarts,¹⁹ Héctor de Paz Martín,¹⁹ María Martín Calero,¹⁹ Riccardo Scarpa,^{5,19} Sergio Fernandez Acosta,¹⁹ William Miguel Hernández Sánchez,¹⁹ Benjamin Siegel,¹⁹ Francisco Francisco Pérez,¹⁹ Himar D. Viera Martín,¹⁹ José A. Rodríguez Losada,¹⁹ Agustín Nuñez,¹⁹ Álvaro Tejero,¹⁹ Carlos E. Martín González,¹⁹ César Cabrera Rodríguez,¹⁹ Jordi Molgó,¹⁹ J. Esteban Rodríguez,¹⁹ J. Israel Fernández Cáceres,¹⁹ Luis A. Rodríguez García,¹⁹ Manuel Huertas Lopez,¹⁹ Raul Dominguez,¹⁹ Tim Gaggstatter,¹⁹ Antonio Cabrera Lavers,¹⁹ Stefan Geier,^{5,19} Peter Peshev,^{5,19} Ata Sarajedini¹

Observations of binary stars containing an accreting black hole or neutron star often show x-ray emission extending to high energies (>10 kilo-electron volts), which is ascribed to an accretion disk corona of energetic particles akin to those seen in the solar corona. Despite their ubiquity, the physical conditions in accretion disk coronae remain poorly constrained. Using simultaneous infrared, optical, x-ray, and radio observations of the Galactic black hole system V404 Cygni, showing a rapid synchrotron cooling event in its 2015 outburst, we present a precise 33.1 ± 0.9 gauss magnetic field measurement in the corona. This measurement is substantially lower than previous estimates for such systems, providing constraints on physical models of accretion physics in black hole and neutron star binary systems.

Observations of accreting black hole systems reveal the existence of an accretion disk coronae (ADC) around the compact object—an energetic electron cloud primarily responsible for nonthermal emission. ADCs are thought to play a role in compact object accretion flows and energetics, especially in black hole binary systems that show relativistic jet outflows. Theoretical models predict that the thick geometry of an ADC leads to the magnetic field configuration required to power jet outflows, and spectral models show that the jet base is identical to the corona in these systems (1–3). However, we have few constraints

on the detailed physical conditions in the jet-launching coronae.

The transient source V404 Cygni (Nova Cygni 1989) was discovered in 1989 (4), and subsequent observations revealed a black hole of 9 to 10 solar mass (M_{\odot}) in a 6.5-day binary orbit (5) with a 0.7 M_{\odot} companion star of spectral type K III; the system is located at a distance of 2.39 kpc (6). V404 Cyg produced an x-ray outburst starting on 15 June 2015 (7, 8), which lasted ~2 weeks. The outburst exhibited behavior including (i) complicated x-ray emission unlike the typical hard/soft states in black hole binaries, including occasional bright flares (9, 10); (ii) long-term correlations in the

optical and x-ray light curves, attributed to thermal x-ray reprocessing (11); (iii) fast red optical flares lasting <1 s, indicating optically thin synchrotron emission from compact regions probably located in a relativistic jet outflow (12); (iv) variable polarization flares indicative of shocks propagating through a relativistic jet outflow (13); and (v) x-ray/radio correlations consistent with jet activity (14).

We present in Fig. 1 multiwavelength observations taken on 25 June 2015, 1 day after the jet-induced polarization flare observations (13). These include near-infrared observations with the Canarias Infrared Camera Experiment (CIRCE) on the 10.4-m Gran Telescopio Canarias (15), three-band optical observations with ULTRAFast CAMERA (ULTRACAM) (12, 16) on the 4.2-m William Herschel Telescope, x-ray observations from the Nuclear Spectroscopic Telescope Array (NuSTAR) satellite (17, 18), and three-band gigahertz radio observations with the Arcminute Microkelvin Imager (AMI) telescope (19). We dereddened the optical/infrared (OIR) data using an estimated extinction $A_V = 4.0$ mag (6, 20). The radio, OIR, and x-ray bands exhibit quasi-independent behaviors. The infrared light curve resembles the optical light curves, including slow modulations of a few minutes with occasional fast flares [which match the jet-related fast flares seen the following day (12)]. The OIR flux levels are >50× higher than the quiescent flux from V404 Cygni as recorded in the Two Micron All Sky Survey (2MASS) catalog (21), indicating that the mass donor star contributes little light on this date, so the emission is dominated by outburst-related processes. The radio emission rises smoothly to 150 millijanskys (mJy)—an increase by a factor of ~10 over ~1 hour, also indicating jet activity (14). The complex x-ray light curve shows two episodes of enhanced x-ray activity coincident with slow modulations in the OIR light curves, as noted in previous studies of this outburst (9, 11). However, other slow OIR modulations exhibit no strong x-ray activity, indicating that the origin of the slow modulations must be more complex than a simple x-ray reprocessing scenario.

We focused on a selected time interval just before 57198.23 Modified Julian Date (MJD), at $t \sim 68$ min in Fig. 1, when there was a sudden flux decay in all bands from infrared to x-ray. This decay came at the end of a ~30-min episode of bright, slowly varying OIR emission accompanied by several rapid x-ray flares. In 4 days of ULTRACAM observations of V404 Cygni around this outburst, this is the only such

¹Department of Astronomy, University of Florida, 211 Bryant Space Science Center, Gainesville, FL 32611, USA. ²Department of Physics and Astronomy, University of Southampton, Highfield, Southampton SO17 1BJ, UK. ³Istituto Nazionale di Astrofisica—Osservatorio Astronomico di Roma, Via Frascati 33, I-00040 Monteporzio Catone, Italy. ⁴Department of Physics and Astronomy, University of Sheffield, Sheffield S3 7RH, UK. ⁵Istituto de Astrofísica de Canarias, 38205 La Laguna, Santa Cruz de Tenerife, Spain. ⁶Department of Physics, University of Warwick, Gibbet Hill Road, Coventry CV4 7AL, UK. ⁷Division of Astrophysics, Department of Physics, University of Oxford, Keble Road, Oxford OX1 3RH, UK. ⁸Institute of Astronomy, University of Cambridge, Madingley Road, Cambridge CB3 0HA, UK. ⁹Space Radiation Laboratory, California Institute of Technology, Pasadena, CA 91125, USA. ¹⁰European Space Astronomy Centre, Operations Department, Villanueva de la Cañada, Madrid, Spain. ¹¹Istituto Nazionale di Astrofisica—Osservatorio Astronomico di Cagliari, via della Scienza 5, 09047 Selargius, Italy. ¹²Istituto de Astrofísica de Andalucía—Consejo Superior de Investigaciones Científicas, E-18008 Granada, Spain. ¹³Unidad Asociada Departamento de Ingeniería de Sistemas y Automática, Universidad de Málaga, 29071 Málaga, Spain. ¹⁴Large Binocular Telescope Observatory, University of Arizona, 933 North Cherry Avenue, Tucson, AZ 85721, USA. ¹⁵Centro de Estudios de Física del Cosmos de Aragón, 44001 Teruel, Aragón, Spain. ¹⁶Department of Physics and Astronomy, University of Texas at San Antonio, One UTSA Circle, San Antonio, TX 78249, USA. ¹⁷National Astronomical Observatory of Japan, 2-21-1 Osawa, Mitaka, Tokyo 181-8588, Japan. ¹⁸Inter-University Centre for Astronomy and Astrophysics, Post Bag 4, Ganeshkhind, Pune-411007, India. ¹⁹Gran Telescopio de Canarias, Cuesta de San José s/n, E-38712, Breña Baja, La Palma, Spain.

*Corresponding author. Email: ydallilar@ufl.edu (Y.D.); eiken@ufl.edu (S.S.E.) †Deceased.

Fig. 1. Multiwavelength light curves of V404 Cygni on MJD 57198 during the 2015 outburst. (A to D)

Observational light curves are shown for (A) three radio frequencies, (B) the infrared Ks band, (C) the r' , g' , and u' optical bands, and (D) 3 to 79 keV x-rays. The optical and infrared bands show slow modulations punctuated by fast red flares. The two optical bumps at ~ 54 and ~ 63 min coincide with bright x-ray flares, whereas the bumps at ~ 42 and ~ 58 min shows very little (if any) x-ray activity, indicating that models invoking simple x-ray reprocessing cannot reproduce the multiwavelength light curve. The cooling event is at ~ 68 min.

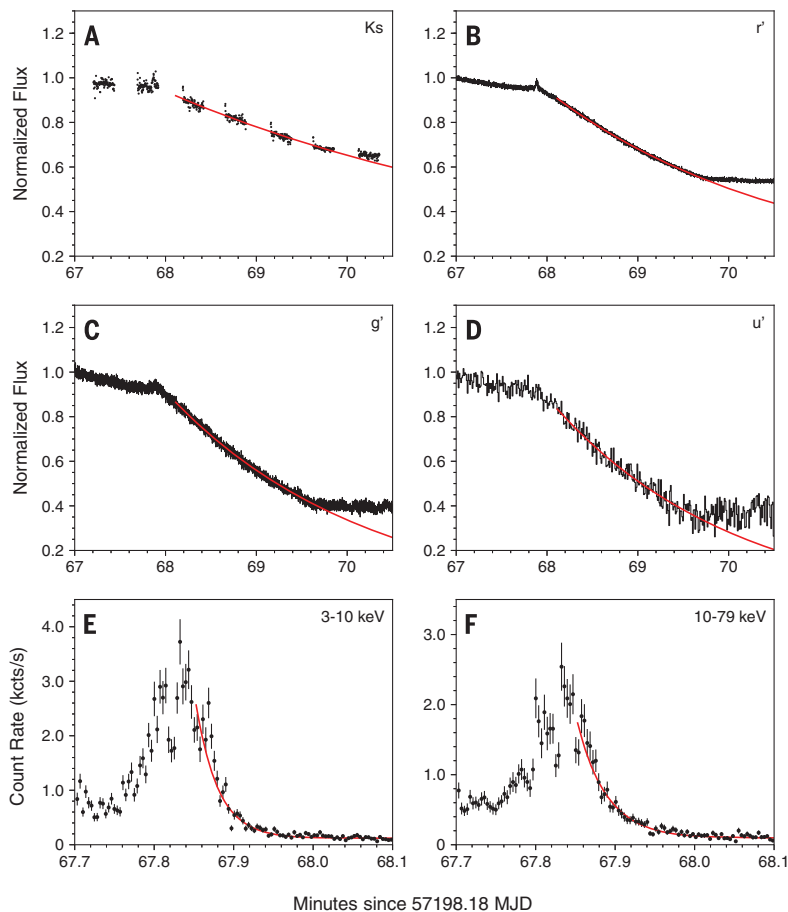
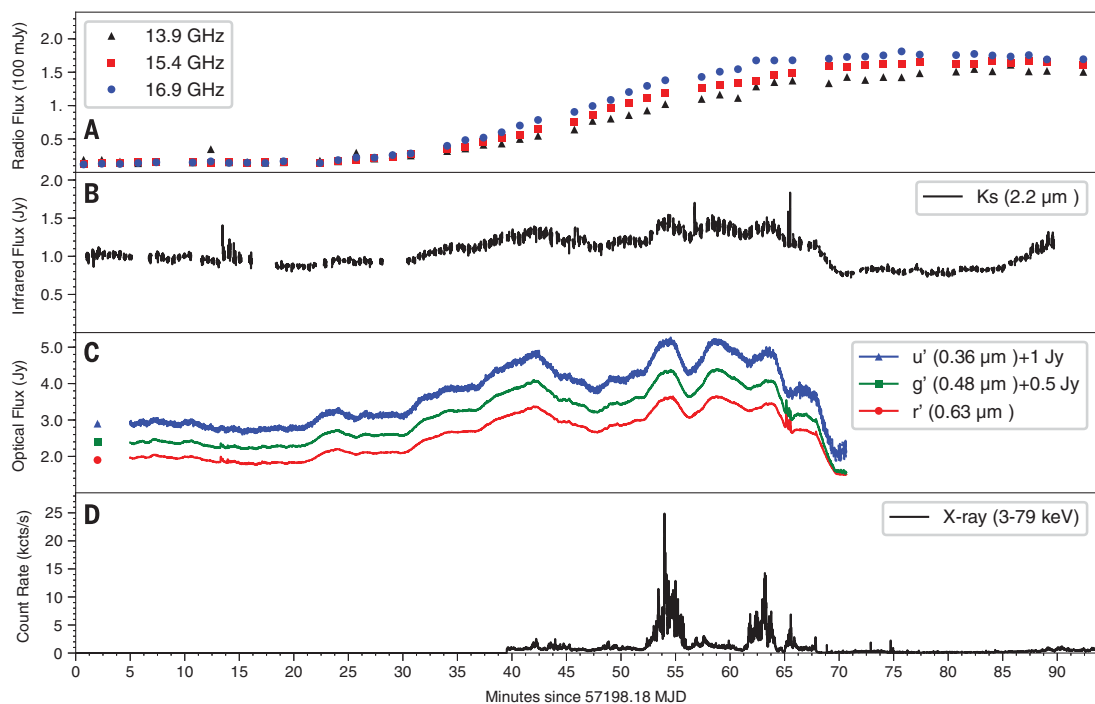


Fig. 2. Simultaneous cooling event decay curves with best-fit exponential models. (A to F) Black lines represent the data, and red lines indicate the best-fit exponential decay profile for the six different energy bands: (A) infrared Ks band; (B), (C), and (D), optical r' , g' , u' band; and (E) and (F), x-ray 3 to 10 keV and 10 to 79 keV. The measured time scales for each are given in table S1.

decay event, so it clearly differs from the rest of the observations [(12), figure 12]. We show this selected time interval in Fig. 2, with the OIR light curves normalized to pre-event fluxes. We modeled the flux profiles with an exponential decay function (Fig. 2 and table S1). The characteristic time scale (τ) puts an upper limit on the size of the emitting region of $R < 1.25 c\tau$ via causality and time-of-flight arguments (20). This approach provides a firm upper limit to the ADC size; hence, considerably smaller values are possible.

To see whether a thermal blackbody could be the origin of the flux during this event, we took the observed color temperature from the ratio of g' and r' bands and calculated an expected thermal emission region size. The required thermal emission region is too large (by more than a factor of 2) to match the observed variability time scale, and we can reject the thermally dominated emission hypothesis with a confidence $>5\sigma$ (fig. S1). This effectively eliminates blackbody emission processes [including x-ray reprocessing on the accretion disk or companion star (11)] as possible origins for the primary OIR emission during the event and indicates that a nonthermal emission process (such as synchrotron or Compton scattering) must be the dominant source of the OIR flux. There is a small OIR flare at the top of the light curve just before the cooling event, which slightly lags the peak of the x-ray emission; this may be a low-amplitude x-ray reprocessing signature or an internal shock in a relativistic jet outflow (fig. S2).

The best-fitting power-law function for $\tau(\nu)$ (table S1) is $\tau \propto \nu^{-0.49 \pm 0.03}$, where ν is the observed radiation frequency and τ represents the decay time scale in each band during the cooling event in Fig. 2 (20). This result is consistent

with the relation $\tau \propto \nu^{-1/2}$ characteristic of synchrotron cooling processes, which is more than five orders of magnitude in frequency (Fig. 3). We eliminated Compton cooling as the origin of the cooling curve in the OIR band on the basis of the magnetic to photon energy densities (20). Although we could not strictly eliminate Compton cooling for the x-rays, whereas thermal or Compton processes could possibly emulate this $\nu^{-1/2}$ frequency scaling, there is no a priori reason to expect them to do so, especially over such a large frequency range. This seems to confirm our conclusion that synchrotron processes dominate this event. Although x-ray measurements are consistent with our best-fitting cooling curve within uncertainties, we observed flattening in the x-ray regime. Therefore, we cannot reject a possible contribution from Comptonization processes in the x-ray band (20).

We calculated individual synchrotron cooling magnetic field measurements from these time scales (table S1), obtaining a best-fitting mean magnetic field (B_0) of 33.1 ± 0.9 G, with reduced $\chi^2_\nu = 0.8$. The individual magnetic field values are all consistent with the mean value within their $\sim 1\sigma$ uncertainties (which are all 2 to 26%). Because a simple single-zone magnetic field model successfully fits all bands simultaneously, over 5 decades in energy for a time-coincident event, the dominant emission mechanism is consistent with a single population of electrons in a common magnetic field. The derived magnetic field has fractional uncertainties $25\times$ smaller than those in GX 339-04 (22). There is no apparent variation in the magnetic field strength during the event, from a decay time scale of <2 s in x-rays to >100 s in the OIR. We estimated a maximum fractional change in the magnetic field of $\Delta B/B_0 < 15\%$ (20). We could use this constraint to investigate possible expansion of the synchrotron-emitting region (because of expansion in a relativistic jet outflow). Magnetic field conservation arguments for adiabatically expanding synchrotron plasmoids generally lead to the conditions $B \propto R^{-\alpha}$, where $1 < \alpha < 2$ and R is the radius of the synchrotron source (23). For the limiting case $\alpha = 1$, any fractional variation in the emitting region size is thus limited to $\Delta R/R < 15\%$. This upper limit suggests a stationary and stable region as the origin of the radiation: a stationary cloud of high-energy electrons confined to a small region. That is the expected disk corona structure for accreting black hole binaries, unlike discrete ejections expanding and moving at relativistic velocity (24).

Minimum energy requirements for synchrotron sources have been used to estimate equipartition magnetic field strengths in extragalactic and Galactic accreting black hole systems. Although there are some well-known caveats to this approach (25), recent studies have demonstrated evidence for charged-particle energies being in equilibrium with the magnetic field energy in a jet system (26). Applying these arguments to the V404 Cygni cooling event,

we derive (20) an equipartition magnetic field strength B_{eq} of

$$B_{\text{eq}} = 651 k^{2/7} (F_\nu/1 \text{ Jy})^{2/7} (\nu/10^{15} \text{ Hz})^{1/7} (\tau/2 \text{ s})^{-6/7} \text{ G} \quad (1)$$

where F_ν is the flux of the source at radiation frequency (ν) and k is defined to be the energy ratio of all charged particles to low-mass charged particles (electrons and positrons) in the system.

We expect the k factor to be >1 for environments with relativistic bulk motions in which the mechanical energy of high-mass charged particles (protons or ions) dominates over the energy of low-mass charged particles. Because there is no clear evidence of bulk motions during the decay of the OIR flux, we assume $k \sim 1$. The derived equipartition field strength of ~ 650 G thus differs by a factor of twenty from the measured value of 33 G, indicating that during this event, V404 Cygni was not in an equipartition energy

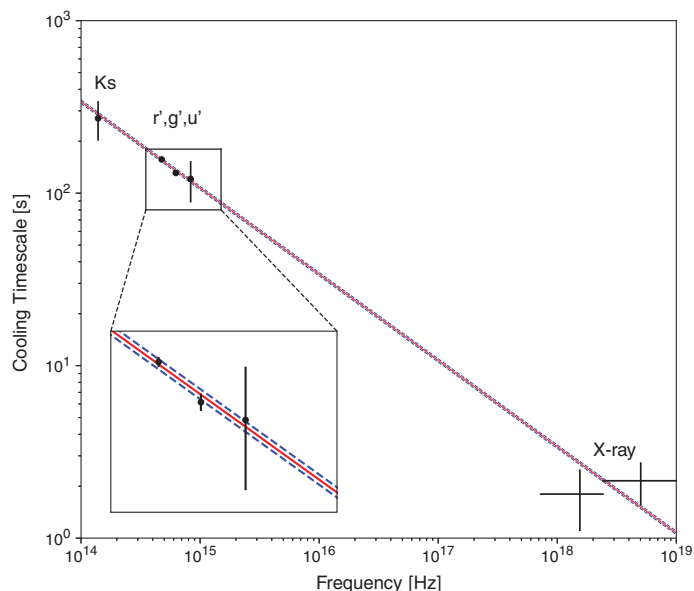


Fig. 3. Cooling time scales as a function of observed radiation frequencies from near-infrared to x-rays. The solid red line shows the best-fitting single-zone magnetic field strength of 33.1 G, with dashed lines at ± 0.9 G uncertainty. The model is fitted over 5 orders of magnitude in frequency; it has a reduced $\chi^2_\nu = 0.8$ and a power-law dependence of $\tau \sim \nu^{-0.49 \pm 0.03}$, which is consistent with the $\nu^{-1/2}$ expected for synchrotron cooling.

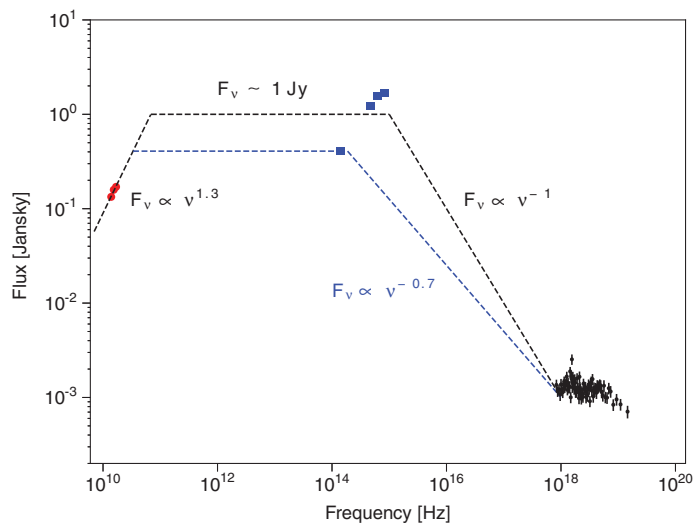


Fig. 4. Spectral energy distribution of the excess emission before the decay event. Fluxes plotted are for the radio (red circles), optical and infrared (blue squares), and x-ray (black crosses) observations (20). We present approximate spectral slopes (dashed lines connecting different energy regimes) as a rough guide to the slopes of apparent spectral breaks.

configuration. We can then derive the energetics in the system: the magnetic field energy $U_B = V u_B \sim 4.0 \times 10^{34} (\tau/2 \text{ s})^3$ ergs, electron kinetic energy $U_e = V u_e \sim 1.1 \times 10^{39} (F_\nu/1 \text{ Jy})(\nu/10^{15} \text{ Hz})^{1/2}$ ergs, and the total energy $U_{\text{tot}} = U_B + U_e \sim 1.1 \times 10^{39}$ ergs (20). Here, V represents the emitting volume, and u_B and u_e are the magnetic field and electron energy densities, respectively. During our observations, the OIR luminosities reach $\sim 10^{37}$ ergs/s, indicating that the overall energy stored in the corona is comparable to about 100 seconds of the system's radiated energy, which is consistent with the rapid variations observed during this outburst being tied to and powered by variations in the accretion luminosity.

We present the overall spectral energy distribution (SED) at the start of the synchrotron cooling event in Fig. 4, along with the corresponding electron energies and densities separately in fig. S3. The SED shown in the OIR regime is the excess flux with respect to the post-decay level [because thermal processes might be dominant in the remaining flux (20)]. The electron Lorentz factors γ range from $\gamma \sim 10$ for the radio to $\gamma \sim 10^3$ for the OIR bands and $\gamma \sim 10^5$ for the x-ray emission, covering the range from mildly relativistic to fully relativistic electrons. The overall distribution at the start of the event is the product of the history of relativistic electron injection into the coronal region at various times during the preceding activity in V404 Cygni, convolved with the relevant energy-dependent cooling time scales. We have no direct insight into the magnetic field properties during this time, nor into the acceleration mechanism populating the corona with relativistic electrons. However, if we assume that the cooling time scales (and thus magnetic field strengths) resemble those measured in the cooling event itself, we can infer possible scenarios. In particular, the x-ray cooling time scales (and associated x-ray-emitting lifetimes of the electrons) would be very short (~ 2 s), so that the x-ray light curve variability would imply multiple electron acceleration/injection episodes over this period, each lasting several minutes and with substantial substructure. The observed correlation of the OIR flux with these events shows that the OIR variability is smoother—as expected for longer-time scale synchrotron cooling of lower-energy electrons. The observed correlations are not necessarily one-to-one between the OIR and x-rays, possibly implying a variable electron energy spectrum at the acceleration site.

Given the complex light curve history, multiple spectral breaks in the flux distribution (and inferred electron energy distribution) at the start of the fading event would arise naturally, as observed in Fig. 4 and fig. S3. For example, the x-ray spectral/energy distribution does not connect smoothly with the OIR region. Again, this is consistent with the much shorter synchrotron time scale for the x-ray-emitting electrons (and thus shorter effective memory of the system), compared with the typical time between injection episodes of 10 to 100 s, which are comparable with or shorter than the expected OIR synchrotron cooling time scales. There is

another spectral break between the OIR and radio emission, as commonly seen in black hole binaries and usually interpreted as increasing self-absorbed synchrotron emission from a radio photosphere with radius $\sim 10^{12}$ to 10^{13} cm (20) containing low-energy electrons. The corresponding light-crossing times are hundreds of seconds, and the presence of a radio photosphere is possibly tied to a large-scale jet feature. This matches both the observed smoothness of the radio light curve and the expected synchrotron opacity at these electron energies/densities for the measured field strength. The OIR emission is expected to be optically thin and thus on the other side of this opacity-induced break.

Our magnetic field measurement provides constraints on jet launching or emission models, especially because it is much lower than previous estimates for other sources: $\sim 10^5$ to 10^7 G for Cyg X-1 (27), $\sim 5 \times 10^4$ G for XTE J1550-564 (28), and $1.5(\pm 0.8) \times 10^4$ G for GX 339-04 (21). A lower field requires an electron energy distribution with higher Lorentz factors (by a factor of 30 or more). Assuming equipartition configuration, it also implies a larger size for the emitting region ($R \propto B_{\text{eq}}^{-7/6}$) (Eq. 1) and lower particle density ($n_e \propto B_{\text{eq}}^{5/2}$) (20). Previous studies have followed a scaling relation between inferred magnetic field and spectral break frequency ν_b in the SED of $B \sim \nu_b L^{-1/9}$ (28, 29). If we associate the OIR peak in Fig. 4 with this break and scale from GX 339-04, we would expect $B \sim 2 \times 10^5$ G for V404 Cygni—which is too high by a factor of ~ 6000 —indicating that the scaling relation may not hold as broadly or simply as previously thought. However, the decay event here only reveals the physical conditions in the jet-launching corona at the time when electron injection/acceleration stops. We have no direct information regarding the process that accelerates the electron population in the first place. A nonexpanding emission region that is physically distinct from the acceleration region in V404 Cygni (and not previously seen in the other sources) could also explain the scaling difference, albeit while requiring that jet base structure varies between sources.

REFERENCES AND NOTES

1. D. L. Meier, *Astrophys. J.* **548**, L9–L12 (2001).
2. S. Markoff, H. Falcke, R. Fender, *Astron. Astrophys.* **372**, L25–L28 (2001).
3. S. Markoff, M. Nowak, S. Corbel, R. Fender, H. Falcke, *Astron. Astrophys.* **397**, 645–658 (2003).
4. F. Makino, *GS 2023+338. Int. Astron. Union Circ.* no. 4782, B. G. Marsden, Ed. (1989).
5. J. Casares, P. A. Charles, D. H. P. Jones, R. G. M. Rutten, P. J. Callanan, *Mon. Not. R. Astron. Soc.* **250**, 712–725 (1991).
6. J. C. A. Miller-Jones *et al.*, *Astrophys. J.* **706**, L230–L234 (2009).
7. S. D. Barthelmy, A. D'ai, P. D'Avanzo, Swift trigger 643949 is V404 Cyg. *The Gamma-ray Coordinates Network Circ.* no. 17929 (2015).
8. H. Negoro *et al.*, MAXI/GSC detection of a new outburst from the Galactic black hole candidate GS 2023+338 (V* V404 Cyg). *The Astronomer's Telegram*. no. 7646 (2015).
9. J. Rodriguez *et al.*, *Astron. Astrophys.* **581**, L9 (2015).
10. T. M. Belloni, in *The Jet Paradigm: From Microquasars to Quasars*, T. Belloni, Ed. (Springer-Verlag, 2010), pp. 53–84.
11. M. Kimura *et al.*, *Nature* **529**, 54–58 (2016).

12. P. Gandhi *et al.*, *Mon. Not. R. Astron. Soc.* **459**, 554–572 (2016).
13. T. Shahbaz *et al.*, *Mon. Not. R. Astron. Soc.* **463**, 1822–1830 (2016).
14. R. M. Plotkin *et al.*, *Astrophys. J.* **834**, 104 (2017).
15. S. S. Eikenberry *et al.*, arXiv:1709.05542 [astro-ph.IM] (16 September 2017).
16. V. S. Dhillon *et al.*, *Mon. Not. R. Astron. Soc.* **378**, 825–840 (2007).
17. F. A. Harrison *et al.*, *Astrophys. J.* **770**, 103 (2013).
18. D. Walton *et al.*, *Astrophys. J.* **839**, L10 (2017).
19. J. T. L. Zwart *et al.*, *Mon. Not. R. Astron. Soc.* **391**, 1545–1558 (2008).
20. Materials and methods are available as supplementary materials.
21. R. M. Cutri *et al.*, 2MASS all-sky catalog of point sources. *VizieR Online Data Catalog*. no. 2246 (2003).
22. P. Gandhi *et al.*, *Astrophys. J.* **740**, L13 (2011).
23. H. C. Spruit, F. Daigne, G. Drenkhahn, *Astron. Astrophys.* **369**, 694–705 (2001).
24. R. Fender, in *The Jet Paradigm: From Microquasars to Quasars*, T. Belloni, Ed. (Springer-Verlag, 2010), pp. 115–142.
25. A. A. Zdziarski, *Mon. Not. R. Astron. Soc.* **445**, 1321–1330 (2014).
26. L. Stawarz *et al.*, *Astrophys. J.* **766**, 48 (2013).
27. M. Del Santo, J. Malzac, R. Belmont, L. Bouchet, G. De Cesare, *Mon. Not. R. Astron. Soc.* **430**, 209–220 (2013).
28. S. Chaty, G. Dubus, A. Raichoor, *Astron. Astrophys.* **529**, A3 (2011).
29. D. M. Russell *et al.*, *Mon. Not. R. Astron. Soc.* **429**, 815–832 (2013).

ACKNOWLEDGMENTS

The near-infrared light curve is based on observations made with the Gran Telescopio Canarias, installed in the Spanish Observatorio del Roque de los Muchachos of the Instituto de Astrofísica de Canarias, in the island of La Palma, during science commissioning of CIRCE. Development of CIRCE was supported by the University of Florida and the National Science Foundation (grant AST-0352664), in collaboration with the Inter-University Centre for Astronomy and Astrophysics. The William Herschel Telescope is operated on the island of La Palma by the Isaac Newton Group in the Spanish Observatorio del Roque de los Muchachos of the Instituto de Astrofísica de Canarias. The ULTRACAM team and P.G. (grant ST/J003697/2) acknowledge the financial support of the U.K. Science and Technology Facilities Council. This research has made use of data obtained with NuSTAR, a project led by the California Institute of Technology, funded by NASA and managed by NASA/Jet Propulsion Laboratory, and has used the NUSTARDAS software package, jointly developed by the Agenzia Spaziale Italiana Science Data Center (Italy) and California Institute of Technology (USA). A.J.C.-T. acknowledges support from the Spanish Ministry Project AYA2015-71718-R. We thank S. Markoff, C. Ceccobello, and T. Maccarone for comments on the scientific discussion. The multiwavelength lightcurves are provided as data file S1, and our derived measurements are listed in table S1. The observational data are available for each instrument: CIRCE at <http://astro.ufl.edu/~ydlillar/Dallilar17/CIRCEraw>; ULTRACAM at https://soton.ac-my.sharepoint.com/personal/pg3e14_soton_ac_uk/Documents/Forms/All.aspx?slid=603d299e%2D704d9%2D4000%2Dbf01%2Dc1708c50f62d&RootFolder=%2Fpersonal%2Fpg3e14%5Fsoton%5Fac%5Fuk%2FDocuments%2Fv404&FolderCTID%3D012000F83BE7EA86B4FE49BECFDA6CEB2B068 (in ULTRACAM pipeline binary format); NuSTAR at <https://heasarc.gsfc.nasa.gov/FTP/nustar/data/obs/01/9/90102007011>; and AMI at www.tau.ac.il/~caltech.edu/kunal/uploads/SWIFT_643949-150625.fits (in radio Flexible Image Transport System format).

SUPPLEMENTARY MATERIALS

www.sciencemag.org/content/358/6368/1299/suppl/DC1
Materials and Methods
Figs. S1 to S3
Table S1
References (30–42)
Data File S1

22 February 2017; accepted 3 November 2017
10.1126/science.aan0249

A precise measurement of the magnetic field in the corona of the black hole binary V404 Cygni

Yigit Dallilar, Stephen S. Eikenberry, Alan Garner, Richard D. Stelter, Amy Gottlieb, Poshak Gandhi, Piergiorgio Casella, Vik S. Dhillon, Tom R. Marsh, Stuart P. Littlefair, Liam Hardy, Rob Fender, Kunal Mooley, Dominic J. Walton, Felix Fuerst, Matteo Bachetti, A. J. Castro-Tirado, Miguel Charcos, Michelle L. Edwards, Nestor M. Lasso-Cabrera, Antonio Marin-Franch, S. Nicholas Raines, Kendall Ackley, John G. Bennett, A. Javier Cenarro, Brian Chinn, H. Veronica Donoso, Raymond Frommeyer, Kevin Hanna, Michael D. Herlevich, Jeff Julian, Paola Miller, Scott Mullin, Charles H. Murphey, Chris Packham, Frank Varosi, Claudia Vega, Craig Warner, A. N. Ramaprakash, Mahesh Burse, Sujit Punnadi, Pravin Chordia, Andreas Gerarts, Héctor de Paz Martín, María Martín Calero, Riccardo Scarpa, Sergio Fernandez Acosta, William Miguel Hernández Sánchez, Benjamin Siegel, Francisco Francisco Pérez, Himar D. Viera Martín, José A. Rodríguez Losada, Agustín Nuñez, Álvaro Tejero, Carlos E. Martín González, César Cabrera Rodríguez, Jordi Molgó, J. Esteban Rodríguez, J. Israel Fernández Cáceres, Luis A. Rodríguez García, Manuel Huertas Lopez, Raul Dominguez, Tim Gaggstatter, Antonio Cabrera Lavers, Stefan Geier, Peter Pessev and Ata Sarajedini

Science **358** (6368), 1299-1302.

DOI: 10.1126/science.aan0249originally published online December 7, 2017

Conditions in a black hole outburst

The binary system V404 Cygni consists of a red giant star orbiting a black hole. In 2015, a surge of accretion by the black hole caused the surrounding plasma to brighten suddenly for the first time since 1989, briefly becoming the brightest x-ray source in the sky. Dallilar *et al.* combined observations from radio, infrared, optical, and x-ray telescopes taken during the outburst. They compared how fast the flux decayed at each wavelength, which allowed them to constrain the size of the emitting region, determine that the plasma within it cooled through synchrotron radiation, and measure the magnetic field around the black hole.

Science, this issue p. 1299

ARTICLE TOOLS

<http://science.sciencemag.org/content/358/6368/1299>

SUPPLEMENTARY MATERIALS

<http://science.sciencemag.org/content/suppl/2017/12/06/358.6368.1299.DC1>

RELATED CONTENT

<http://science.sciencemag.org/content/sci/360/6386/eaat9270.full>

REFERENCES

This article cites 29 articles, 0 of which you can access for free
<http://science.sciencemag.org/content/358/6368/1299#BIBL>

Use of this article is subject to the [Terms of Service](#)

PERMISSIONS

<http://www.sciencemag.org/help/reprints-and-permissions>

Use of this article is subject to the [Terms of Service](#)

Science (print ISSN 0036-8075; online ISSN 1095-9203) is published by the American Association for the Advancement of Science, 1200 New York Avenue NW, Washington, DC 20005. 2017 © The Authors, some rights reserved; exclusive licensee American Association for the Advancement of Science. No claim to original U.S. Government Works. The title *Science* is a registered trademark of AAAS.